Electric Power Systems Research 160 (2018) 56–62

Contents lists available at ScienceDirect

Electric Power Systems Research

journal homepage: www.elsevier.com/locate/epsr

Wavelet analysis of a memristor emulated model proposed for compact fluorescent lamp operated systems

Y. Babacan [a], C.P. Uzunoğlu [b,*], S. Cekli [c], F. Kaçar [b], M. Uğur [b]

[a] Electrical and Electronics Engineering Department, Erzincan University, Erzincan, Turkey
[b] Electrical and Electronics Engineering Department, Istanbul University, Istanbul, Turkey
[c] Computer Engineering Department, Maltepe University, Istanbul, Turkey

ARTICLE INFO

Article history:
Received 6 June 2017
Received in revised form
17 December 2017
Accepted 3 February 2018

Keywords:
Memristor
Compact florescence lamp
Wavelet analysis
Total harmonic distortion

ABSTRACT

Compact fluorescent lamps (CFLs) are widely employed in lighting systems thanks to their energy efficient characteristics. In contrast to incandescent lamps, CFLs have highly non-linear current–voltage characteristics and exhibit harmonic distortions during their operation. Although nonlinearity and accelerated harmonic effects may cause disturbance in power networks, CFLs are frequently preferred due to their low energy consumption. In this study a test set-up is operated for investigating non-linear characteristics of commercially available CFLs. During these tests non-linear current and voltage waveforms of CFLs are analyzed via oscilloscope and compared with the proposed memristor emulator circuit output waveforms. The non-linear characteristics of CFLs are accurately modelled by proposed memristor emulator circuit, which has a tunable threshold property. To obtain proper comparison wavelet analysis is conducted for current waveforms of CFLs and memristor emulator circuit. The wavelet analysis is an efficient tool for processing non-linear signals, which are prone to display high frequency distortions. In addition to wavelet analysis, the Fourier Transform (FFT) characteristics and total harmonic distortion (THD) levels are also analyzed for correlation of CFLs and proposed memristor.

© 2018 Elsevier B.V. All rights reserved.

1. Introduction

In recent applications, the energy efficiency of electrical networks has become main interest since better utilization of these systems satisfy reduced consumer costs, improved signal quality and reduced environmental effects. Compact Fluorescent Lamps (CFLs) have recently been introduced to market due to their much more efficient characteristics in comparison with conventional incandescent bulbs [1–3].

CFLs can reduce electricity consumption up to seventy-five percent (in watts) compared to conventional incandescent bulbs, however increased efficiency comes with some drawbacks. CFL requires electronic ballast to initiate the operation, which naturally produces disturbing harmonic currents [4]. Increased harmonic currents causes reduced system signal quality and distorted voltage–current waveforms [5]. Increased total harmonic distortions (THD) may initiate chaotic state of the power system, which is quite common memristive systems [6].

Chua announced memristor, which was introduced as fourth passive circuit element in 1971 and 1976 [7,8]. Recently after the first announcement of memristor Strukov et al. have experimentally fabricated memristor [9]. As a fourth basic circuit element, memristor (resistor with memory), is presented as fundamental circuit component which defines charge and flux interactions contrary to other passive components.

Memristors exhibit pinched hysteresis loop when a periodic sinusoidal signal applied, and display linear characteristics at higher frequencies. The memristor resistance (memristance) depends on the input signal polarity and consequently memristance increases or decreases with the reversed polarity of the system. In order to emphasize importance of memristive systems, some useful properties of memristor such as passive circuit component structure with two terminals, hysteresis loop in the I–V (current–voltage) plot and nonlinear q–φ curve, apparent at small scales and no storage of energy are presented.

Many researchers have analyzed memristor and memristor based circuit system designs after its physical fabrication. SPICE models [10–13] and emulators [14–20] are developed to emulate memristors to employ with other circuit components. Memristors are suitable to design and simulate chaotic circuits because of their nonlinear behavior. For this purpose, there are various studies on

* Corresponding author.
E-mail address: polat@istanbul.edu.tr (C.P. Uzunoğlu).

https://doi.org/10.1016/j.epsr.2018.02.001
0378-7796/© 2018 Elsevier B.V. All rights reserved.

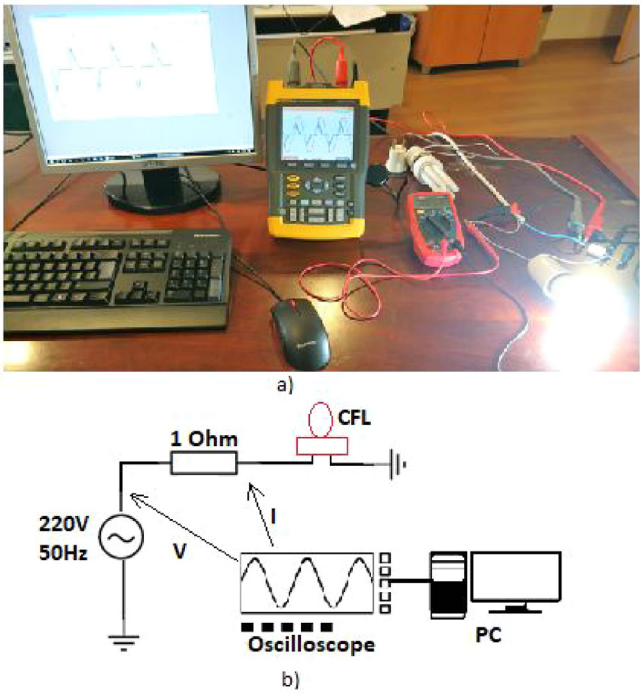


Fig. 1. CFL test setup (a) experimental setup (b) block diagram.

the chaotic behavior of memristor and its circuit applications have been conducted [21–24].

In this study, proposed memristor model is investigated and compared with employed CFLs in terms of non-linear operation. The I–V characteristics of CFLs were experimentally recorded and analyzed. THD level and FFT plots were compared. The proposed memristor emulator circuit's I–V characteristics, THD level and FFT plot were investigated and CFL simulation with proposed system is verified. In order to express the performance of the proposed memristor model, wavelet analysis is proposed for investigating nonlinear characteristics.

It is quite a challenging task to analyze non-linear signals by using conventional methods such as FFT method since this method naturally analyzes total signal frequency components instead of focusing on small fragments of the signal. In this study due to nonlinear and harmonic distortions of memristor and CFL signals, continuous wavelet transform (CWT) technique [25] is proposed for determination of non-linearity (chaoticness) of these signals. In literature, wavelet analysis has different application fields such as biomedical, mechanics, telecommunications, radar, compressing etc. [25–29].

2. Test setup

In order to investigate CFL characteristics the test setup, which is given in Fig. 1, is employed. As a power supply, single-phase rated 220 V–50 Hz electrical distribution network is used. Current and voltage waveforms were recorded by high speed oscilloscope. Current recordings were collected through a 1 Ω resistor (voltage signal represents current signal for a 1 Ω resistor) to observe current signal on oscilloscope. Voltage readings were obtained from phase voltage of the system.

In this study 18 W (stick bulb shape) and 23 W (spiral bulb shape) CFLs are employed and named as CFL1 and CFL2 respectively for ethical issues. Commercially available CFL1 and CFL2 lamps are investigated and corresponding signal waveforms are recorded. Signal recordings are transferred to computer for processing.

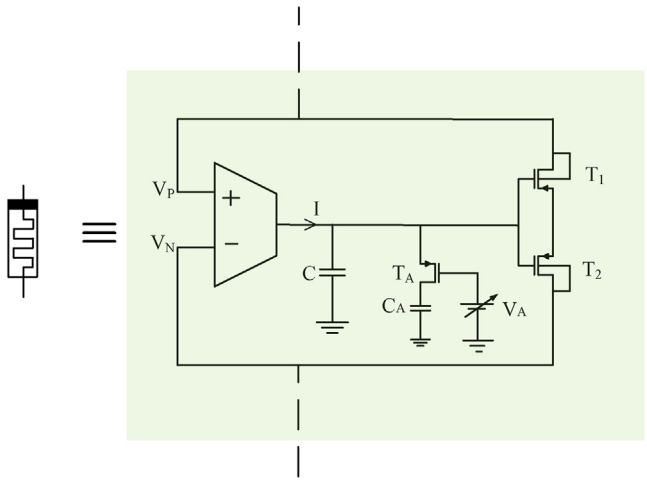


Fig. 2. Memristor circuit with tunable threshold.

3. Memristor emulator circuit and experimental CFL results

Strukov et al. from Hewlett Packard presented a simple mathematical memristor model [9]. Current–voltage relationship can be expressed by,

$$V(t) = R(t)\,i(t) = \frac{d\varphi}{dq}\,i(t) \tag{1}$$

Here, q and φ denote the charge and flux, respectively. Memristance is the ratio of flux to charge and the memristance can be changed by applying voltage or current signal across the memristor. The current–voltage relationship is,

$$V(t) = \left[R_{ON}\frac{x(t)}{D} + R_{OFF}\left(1 - \frac{x(t)}{D}\right)\right] i(t) \tag{2}$$

R_{ON} and R_{OFF} values are low and high resistance, respectively, D denotes the thickness of memristor, x denotes the thickness of doped area in the memristor and μV is the electron mobility. The variation of x value plays important role for memristor characteristics which is defined by [9],

$$\frac{dx(t)}{dt} = \mu_V \frac{R_{ON}}{D} i(t) \tag{3}$$

Current-mode structures are useful tools for circuit designers to obtain low power consumptions. For this purpose, the current mode based memristor emulator circuit is proposed as shown in Fig. 2. This circuit consists of only one voltage controlled current source element (operational transconductance amplifier-OTA), two capacitors, three MOSs and one voltage source. Gates of the MOSs are driven by the capacitor voltage. The capacitors are charged and discharged by OTA. The relationship of input voltage and output current of OTA is given by,

$$I = g_m(V_P - V_N) \tag{4}$$

Here, *gm* is transconductance of OTA circuit element and output current can be controlled for both input voltages and *gm* value. The threshold of memristor can be changed by using V_A voltage source.

The VA voltage source is directly connected to the gate of TA transistor and memristor threshold voltage can be controlled by changing the VA voltage source. The current–voltage curves with various threshold barriers are shown in Fig. 3. Besides the behavior of memristor can be controlled by changing the values of gm, capacitors and dimensions of transistors. For instance, the memristance (the resistance of memristor) can be increased or decreased when the dimensions of transistor is decreased or increased, respectively. The operation frequency of memristor can be controlled by

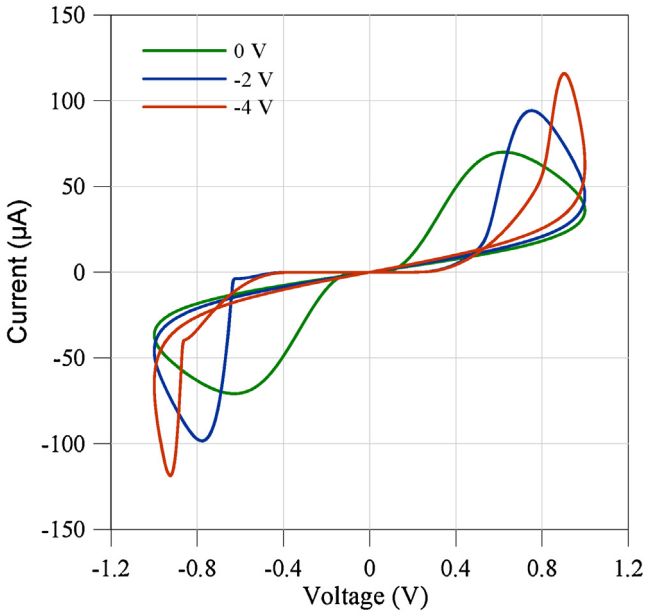


Fig. 3. Voltage–current characteristics of memristor with various V_A voltage source. Here, gm of OTA = 10 μS, C = 100 pF, C_A = 5 nF, $(W/L)T_A = (W/L)T_1 = (W/L)T_2$ = 1 μm/1 μm.

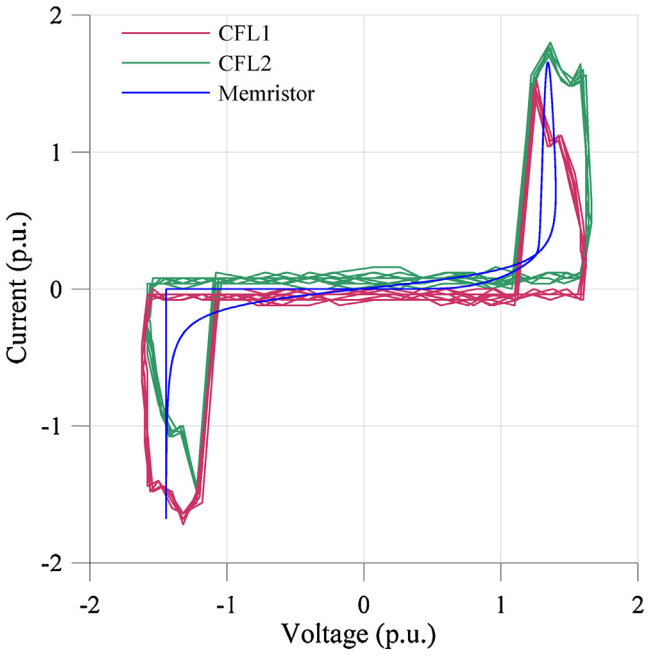


Fig. 4. Current–voltage characteristics of CFL1, CFL2 and memristor emulator circuit.

changing the capacitor values. In summary, previous studies on memristors [10–20] are lack of the both fully floating and fully controllable characteristics but the proposed circuit can be used in various applications because of its versatile controllable structure.

The experimental voltage–current waveforms for CFL1 and CFL2 at 50-Hz operating frequency have been shown in Fig. 4. The simulated current–voltage characteristic of memristor emulator circuit when applied with 1 V and 50 Hz sinusoidal input signal is also given in Fig. 4.

In order to depict all the voltage–current waveforms in one figure the voltage and current values are given in p.u. The simulated and recorded current–voltage waveforms exhibit similar

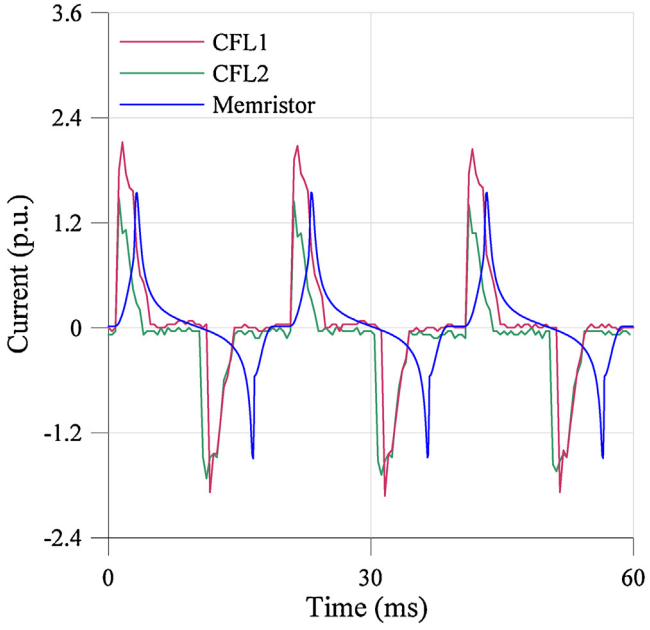


Fig. 5. The current signal of CFL1, CFL2 and memristor emulator circuit.

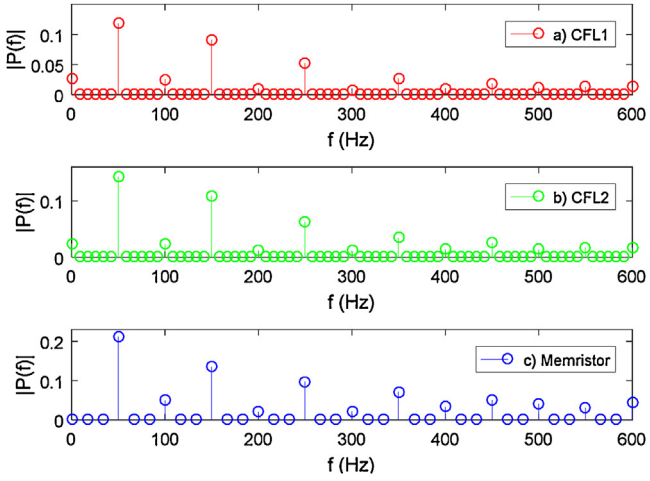


Fig. 6. Fourier transform of (a) CFL1 (b) CFL2 and (c) memristor emulator circuit current signals.

characteristics obviously. It is noted that CFLs produce harmonic currents, which result in nonlinear system responses. The current waveforms of simulated memristor and analyzed CFLs are given in Fig. 5. The characteristics parameters of the proposed model are chosen according to current–voltage variations (hysteresis), which are important signatures of memristors. Current–Voltage sketch of memristor is quite similar to CFL application where nonlinear system operation is observed. Besides it is also quite obvious that memristor model is ideal and hence does not contain any noises contrary to real CFL application.

Total harmonic distortion (THD) is useful tool for analyzing harmonic impact produced on the system. In order to calculate THD the following equation is employed.

$$THD_{current} = \frac{\sqrt{I_2^2 + I_3^2 + I_4^2 + \ldots.}}{I_1} \quad (5)$$

The THDs for CFL1 and CFL2 lamps are calculated as 59% and 55% respectively. The frequency spectrum (FFT) of these CFLs and proposed memristor circuits current signals are given in Fig. 6

respectively. The frequency spectrum exhibit quite similar characteristics for CFLs and proposed memristor model where 3th, 5th, 7th and following order components are quite definitive.

Variations of harmonic frequency components are expected since calculated THDs are quite significant. The THD for proposed memristor circuit is calculated as 60%, which is approximately same with investigated CFLs. Frequency spectrums of analyzed CFLs and proposed memristor depict similar properties and layouts. THD calculations are conducted by using 600 Hz bandwidth (11th order harmonic) which is in accordance with frequency spectrum. The spectrum is analyzed for 600 Hz bandwidth since higher order harmonics have similar trends with the lower frequency components.

4. Wavelet analysis

Wavelet analysis is an efficient algorithm for non-linear and distorted signals which have sharp oscillations and spikes. The wavelet transform is used for transforming a time signal from time domain into the time-scale domain within a definite time period by using functions which are called wavelets (wave-like transition) [29]. A specific type of wavelet transform is mainly based on a specific wavelet function, which is defined as "mother wavelet" [25]. The wavelet transform is achieved by transforming original time signal by employing shifted and scaled combinations of mother wavelet functions. The $\psi(t)$ parameter is a mother wavelet function which is given in a complex-valued vector space for time signals. In general complex-valued signals with finite energy satisfy following equation.

$$\int_{-\infty}^{\infty} \psi^2(t)\,dt < \infty \tag{6}$$

Eq. (6) exhibits finite energy condition for a given function. The second condition for wavelet transform is the smoothness capability (Eq. (7)) of the function in frequency domain where the Fourier Transform of given function for zero frequency is zero ($FFT\Psi(0) = 0$). The functions that are capable of satisfy these conditions are named mother wavelet functions or base functions [25,29].

$$C\psi = 2\pi \int_{-\infty}^{\infty} \frac{|FFT\Psi|^2}{|\omega|} d\omega < \infty \tag{7}$$

The continuous wavelet transform of a specific signal x (t) can be evaluated by using the chosen mother wavelet function.

$$CWT_x^{\psi}(\tau, s) = \frac{1}{\sqrt{|s|}} \int x(t)\,\psi^*\left(\frac{t-\tau}{s}\right) \tag{8}$$

In the transformation equality the ψ^* denotes complex conjugate of mother wavelet function and transformation is achieved on the plane which is characterized by τ and s parameters ($\tau, s \in R$ and $s > 0$). The τ is named dilation parameter and it defines time-shift of a function. The s is called translation parameter and the scaling of the continuous wavelet transform is based on this parameter [30]. In this study, a Meyer-type mother wavelet function is chosen since it has quite quick response time and capable of handling high frequency characteristics [31,32].

During the tests the non-linearity of the CFLs are observed on distorted current signals. For this purpose, the CWTs of current signals for both CFLs and memristor circuit are investigated. The CWT coefficients of CFL1 current signal versus time is given in Fig. 7.

CWT coefficients signal represents distortions on a given signal. Due to the distortions of non-linear operating characteristics of CFL, sharp spikes and quick fluctuations are expected on the CWT signal. The CWT coefficients of CFL2 current signal is given in Fig. 8. The CWT analysis of CFL2 exhibits quite similar characteristics with the CFL1 lamp where accelerated fluctuations observed around zero amplitude. In order to investigate chaoticness (complexity) of the CFL, which is simulated by using memristor emulator circuit, the CWT analysis of memristor emulator circuit is given in Fig. 9. It is

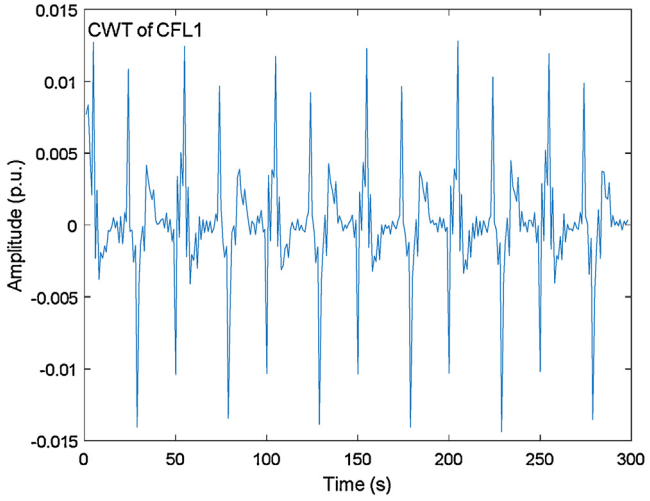


Fig. 7. CWT analysis of CFL1 current signal.

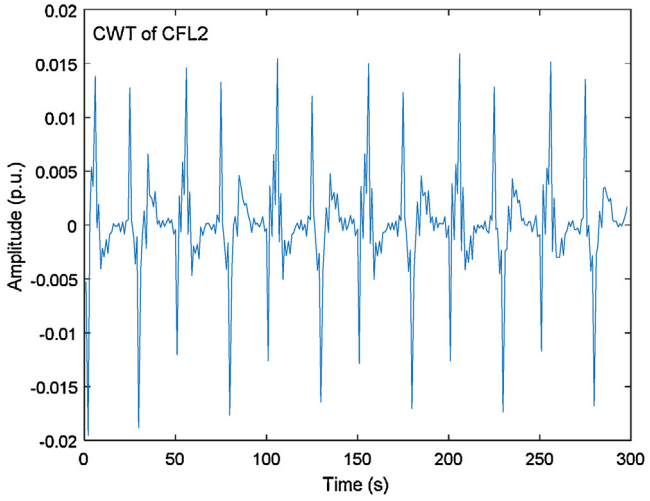


Fig. 8. CWT analysis of CFL2 current signal.

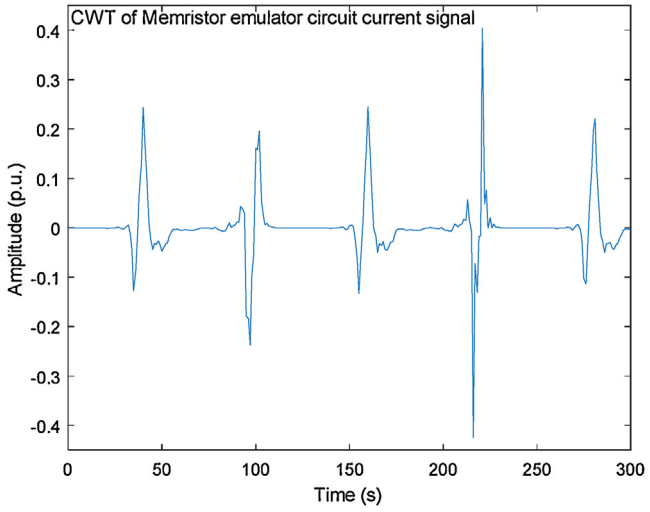


Fig. 9. CWT analysis of memristor emulator current signal.

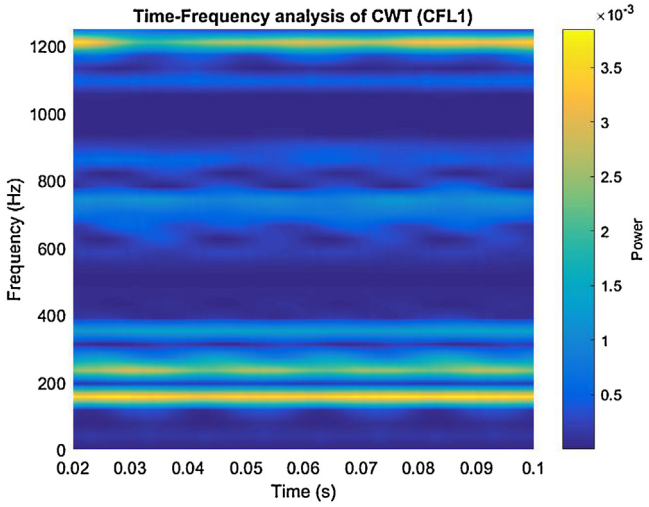


Fig. 10. The time–frequency analysis of CWT (CFL1).

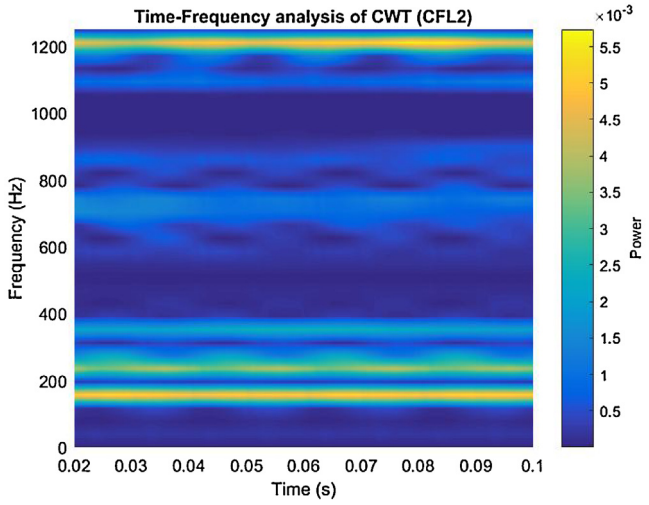


Fig. 11. The time–frequency analysis of CWT (CFL2).

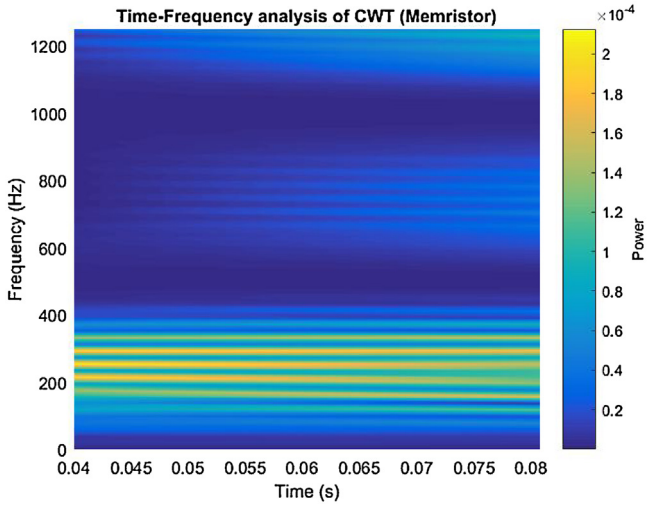


Fig. 12. The time–frequency analysis of CWT (memristor emulator).

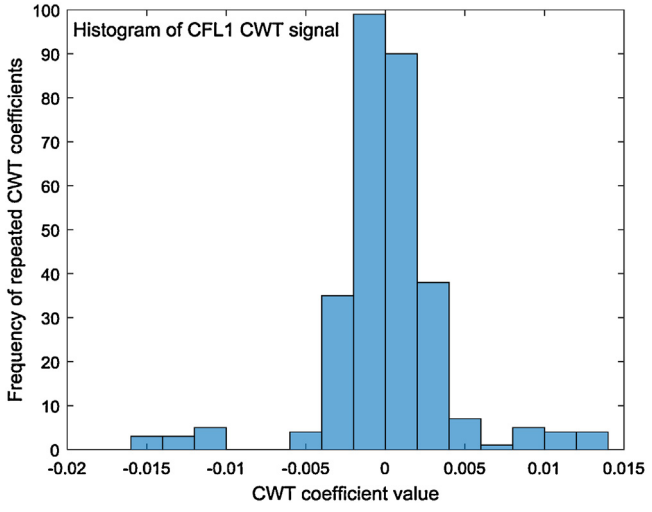


Fig. 13. Histogram of CFL1 CWT signal.

clear from Fig. 9 that the noise exhibits sharper formation than the CFL noises.

Proposed circuit only contains model distortions which is produced artificially by SPICE model. On the other hand, the tested CFLs display measurement noises in addition to CFL characteristics. For these purpose the additional noises of the real CFLs should be taken into account. The CWT analysis of CFLs contain much more fluctuations in contrast to proposed memristor circuit since real world noises are occurred as the bottleneck signal waveforms.

In order to investigate time based frequency characteristics of proposed model, time–frequency analysis is conducted for wavelet coefficients. In this analysis the wavelet coefficients are mapped into time–frequency relations based on their signal characteristics. The time based frequency transitions are investigated in terms of signal power on that frequency spectrum. The time–frequency analysis of CFL1's wavelet coefficients is given in Fig. 10.

The frequency spectrum is mainly distributed up to 400 Hz range over time uniformly. Some additional components are observed (non-uniform) approximately around 700 Hz and 1.2 kHz. These readings indicate that how uniformly power spectrum distributed over time. The time–frequency analysis of CFL2's wavelet coefficients is given in Fig. 11.

The frequency spectrum is quite similar with CFL1 which is also distributed up to 400 Hz efficiently over time (non-uniform) and exhibit additional components around 700 Hz and 1.2 kHz. The time–frequency analysis of proposed memristor model's wavelet coefficients is given in Fig. 12.

In the time–frequency analysis of memristor it has been observed that the main components are distributed up to 400 Hz over time (uniformly) which is quite common with CFLs. These distributions are extremely sharp in contrast to CFLs due to the ideal modelling of SPICE. Since the theoretical proposed model is noise and measurement error free, these results are expected. Additionally, non-uniform distributions around 700 Hz and 1.2 kHz are observed like CFLs.

In addition to CWT analysis, the histograms of CWT signals are analyzed for comparison purposes. The histogram of CFL1 CWT signal is given in Fig. 13.

The histogram analysis defines the frequency of oscillations and sharp transitions of the time signal. In other words, how frequently CWT coefficients are observed on a given signal. The histogram of CFL2 CWT signal is given in Fig. 14.

The histogram analysis defines the frequency of oscillations and sharp transitions of the time signal. As long as wavelet coefficients are related with the noise observed on a time series signal, the number of repeated coefficients can be used as a measure of noise components and their variations on that signal. The histograms reveal that the distributions are similar (distributed mainly around

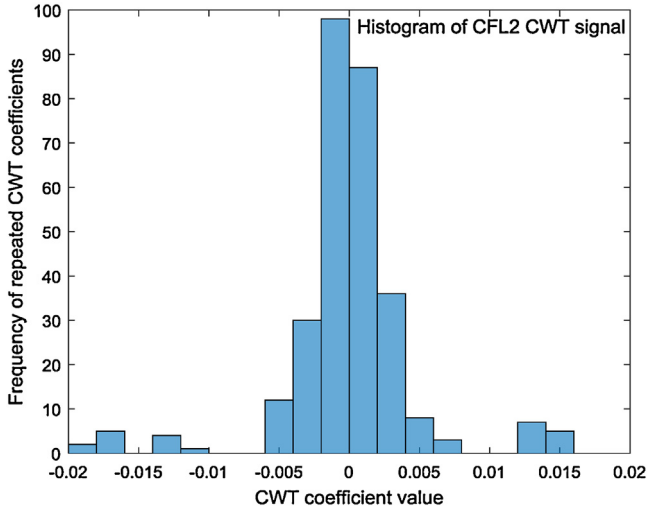


Fig. 14. Histogram of CFL2 CWT signal.

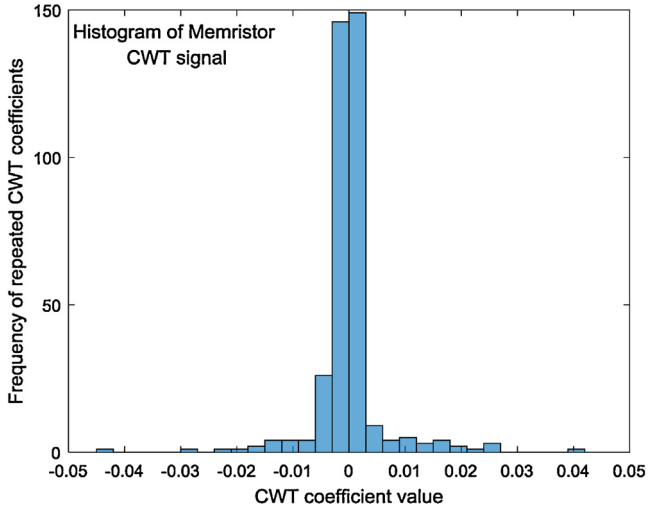


Fig. 15. Histogram of memristor emulator CWT signal.

zero) in terms of fluctuations. The non-linear operation of proposed memristor emulator also satisfies similar histogram characteristics which is given in Fig. 15. In real world scenario the observed CFLs exhibit relatively more distributed characteristics around zero than the proposed memristor emulator. The main reason of this phenomenon is based on the measurement noises of the real CFLs which promote distributed histogram characteristics. Proposed memristor model (simulation) does not contain ambient noises which may lead to much more similar histograms however supplied histogram sketch of memristor display quite satisfying characteristics compared to the CFL histograms.

5. Conclusions

In this study, non-linear operation characteristics of CFL's are modelled by using tunable threshold and floating memristor emulator circuit efficiently. During the tests two similar CFL type (CFL1 & CFL2) lamps are employed. Current and voltage waveforms of these CFLs are acquired and processed. Although CFLs are much more efficient than the incandescent type bulbs, they display nonlinear load characteristics and hence increased harmonic currents. Increased harmonic components cause increased THD and distorted waveforms. The current–voltage characteristics of the proposed memristor reveals similar characteristics to the current–voltage curves of the tested CFLs. Various threshold voltages of the proposed memristor emulator can be changed by tuning only one voltage source which is superior to other emulators. With novel floating and fully controllable characteristics, the proposed memristor emulator circuit is capable of simulating various applications thanks to its versatile controllable structure. The frequency spectrums and calculated THDs of CFLs and memristor circuit display quite similar characteristics. In addition, wavelet analysis is conducted for both CFLs and memristor emulator circuit, which have non-linear waveforms and repeated fluctuations in common. CWT coefficient evaluations which exhibit time behaviors of analyzed nonlinear signals based on frequency knowledge on that signal are compared. The time–frequency characteristics of CWT coefficients exhibit quite similar spectrums over time axis for CFLs and memristor emulator. The histogram analysis is conducted for defining the frequency of oscillations of the CWT signals in which close comparison results obtained consequently. The proposed memristor emulator with tunable threshold can be employed for modelling CFLs and various systems with nonlinear characteristics efficiently.

Acknowledgment

This work was supported by Erzincan University Research Fund with the project code FBA-2017-466. The authors would like to thank Erzincan University Research Fund for this financial support.

References

[1] L.R. Nerone, Analysis and design of a self-oscillating class e ballast for compact florescent lamps, IEEE Trans. Ind. Electron. 48 (1) (2001) 151–160.
[2] M.A. Shafi, R.A. McMahon, S. Weier, Investigation of losses in commercially available self-resonant ballasts for compact florescent lamps, in: Power Electronics Specialists Conference, June17–21, 2007, pp. 3100–3105.
[3] S. Hussain, A. Mohamed, K. Mohamed, Sensitivity of compact fluorescent lamps during voltage sags: an experimental investigation, WSEAS Trans. Power Syst. 5 (2010) 22–31.
[4] R.R. Verderber, O.C. Morse, W.R. Aling, Harmonics from compact fluorescent lamps, in: Industry Application Society Annual Meeting, Conference Record, September 28 –October 4, Dearborn, 1991, pp. 1853–1858.
[5] J.J. Gutierrez, P. Saiz, I. Azcarate, L.A. Leturiondo, K. Redondo, S. Ruiz de Gauna, Digna M. Gonzalez-Otero, Sensitivity of modern lighting technologies at varying flicker severity levels, Int. J. Electr. Power Energy Syst. 92 (2017) 34–41.
[6] C.P. Uzunoglu, Y. Babacan, F. Kacar, M. Ugur, Modeling and suppression of chaotic ferroresonance in a power system by using memristor-based system, Electr. Power Comp. Syst. 44 (6) (2016) 638–645.
[7] L.O. Chua, Memristor — the missing circuit element, IEEE Trans. Circuit Theory 18 (1971) 507–519.
[8] L.O. Chua, S.M. Kang, Memristive devices and systems, Proc. IEEE (1976) 209–223.
[9] D.B. Strukov, G.S. Snider, D.R. Stewart, R.S. Williams, The missing memristor found, Nature 453 (2008) 80–83.
[10] Z. Biolek, D. Biolek, V. Biolkova, SPICE model of memristor with nonlinear dopant drift, Radioengineering (2009) 210–214.
[11] S. Benderli, T.A. Wey, On SPICE macromodelling of TiO_2 memristors, Electron. Lett. 10 (4) (2009) 377–379.
[12] Y. Zhang, X. Zhang, J. Yu, Approximated SPICE model for memristor, International Conference on Communications, Circuits and Systems, ICCCAS (2009).
[13] Y. Chen, X. Wang, Compact modeling and corner analysis of spintronic memristor, Int. Symp. Nanoscale Architect (2009) 7–12.
[14] S. Shin, et al., Compact circuit model and hardware emulation for floating memristor devices, IEEE Circuits Syst. Mag. (2013) 42–55.
[15] Z. Kolka, D. Biolek, V. Biolkova, Hybrid modelling and emulation of mem-systems, Int. J. Numer. Model. Electron. Netw. Dev. Fields (2012) 216–225.
[16] R. Mutlu, E. Karakulak, Emulator circuit of TiO_2 memristor with linear dopant drift made using analog multiplier, Electrical, Electronics and Computer Engineering (ELECO) (2010) 380–384.
[17] H. Kim, M. Sah, P. Yang, C.S. Cho, L.O. Chua, Memristor emulator for memristor circuit applications, IEEE Trans. Circuits Syst. I Regul. Papers 59 (10) (2012) 2422–2431.
[18] C.P. Uzunoglu, Y. Babacan, S. Cekli, F. Kacar, M. Ugur, Modelling of compact fluorescent lamp characteristics using memristor emulator circuit, in:

International Conference on Memristive Materials, Devices & Systems, Athens, Greece, 2017.
[19] A. Yesil, Y. Babacan, F. Kacar, A new DDCC based memristor emulator circuit and its applications, Microelectron. J. 45 (3) (2014) 282–287.
[20] Y. Babacan, F. Kacar, Floating memristor emulator with subthreshold region, Analog Integr. Circuits Signal Process. 90 (2) (2016) 471–475.
[21] B. Muthuswamy, P.P. Kokate, Memristor-based chaotic circuits, IETE Tech. Rev. (2009) 417–429.
[22] B. Muthuswamy, Implementing memristor based chaotic circuits, Int. J. Bifurc. Chaos (2010) 1335–1350.
[23] E. Lehtonen, M. Laiho, J. Poikonen, A chaotic memristor circuit, 2010 12th International Workshop on Cellular Nanoscale Networks and their Applications (CNNA) (2010).
[24] T. Driscoll, Y.V. Pershin, D.N. Basov, M. Di Ventra, Chaotic memristor, Appl. Phys. A (2011) 885–889.
[25] D.T. Lee, A. Yamamoto, Wavelet analysis: theory and applications, Hewlett Packard J. 45 (1994) 44.
[26] M.J. Medley, G.J. Saulnier, P.K. Das, Applications of the wavelet transform in spread spectrum communications systems, SPIE's International Symposium on Optical Engineering and Photonics in Aerospace Sensing (1994) 54–68.
[27] Y.S. Oh, J. Han, G.H. Gwon, D.U. Kim, C.H. Kim, Development of fault detector for series arc fault in low voltage DC distribution system using wavelet singular value decomposition and state diagram, J. Electr. Eng. Technol. 10 (3) (2015) 766–776.
[28] M. Rucka, K. Wilde, Application of continuous wavelet transform in vibration based damage detection method for beams and plates, J. Sound Vib. 297 (3–5) (2006) 536–550.
[29] S.M.H. Hosseini, P.R. Baravati, Partial discharge localization based on detailed models of transformer and wavelet transform techniques, J. Electr. Eng. Technol. 10 (3) (2015) 1019–1101.
[30] A. Cohen, J. Kovacevic, Wavelets: the mathematical background, Proc. IEEE 84 (4) (1996) 514–522.
[31] Y. Meyer, Wavelets-algorithms and Applications, vol. 142, Society for Industrial and Applied Mathematics Translation, 1993.
[32] C.P. Uzunoglu, Investigation of degradative signals on outdoor solid insulators using continuous wavelet transform, J. Electr. Eng. Technol. 11 (3) (2016) 683–689.